Journal of Convex Analysis
Volume 28 (2021), No. 2, 535–548
https://doi.org/10.68381/jca28030

# A Numerical Study of the Jerky Crack Growth in Elastoplastic Materials with Localized Plasticity

**Gianni Dal Maso, Luca Heltai**
*SISSA, Via Bonomea 265, 34136 Trieste, Italy*
*dalmaso@sissa.it, luca.heltai@sissa.it*

*Dedicated to Umberto Mosco on the occasion of his 80th birthday.*

Received: April 27, 2020
Accepted: May 6, 2020

We present a numerical implementation of a model of quasi-static crack growth in linearly elastic-perfectly plastic materials. We assume that the displacement is antiplane, and that the cracks and the plastic slips are localized on a prescribed path. We provide numerical evidence of the fact that the crack growth is intermittent, with jump characteristics that depend on the material properties.

*Keywords:* Fracture mechanics, plasticity, quasistatic evolution, rate-independent problems, finite element method.

*2010 Mathematics Subject Classification:* 49K10, 35J05, 35J25, 65N22, 74A45, 74C05.

## 1. Introduction

Models of quasi-static crack growth in elasto-plastic materials provide a description of fracture which is more accurate with respect to the classic purely brittle approach (see, for example, [11, 14, 15] and, for a numerical treatment, [7, 13, 18]). Indeed, in real materials the crack tip is always surrounded by a process zone where several nonlinear phenomena occur, among which plastic slip is one of the most relevant.

The case of crack growth in linearly elastic–perfectly plastic materials in the small strain regime was considered in [5] in the framework of the energetic approach to rate independent systems (for which we refer to [12] and the references therein).

Recent developments [6] have shown that in this model the crack growth is jerky. To be precise, the mathematical proof of this result has been obtained in a simplified setting in the antiplane case in dimension two, where both the plasticity and the crack are confined on a prescribed path. This jerky behavior is in agreement with experimental results [8, 10] and with numerical evidence (see, for example, [3, 13]).

In this work we provide a numerical implementation of the model introduced in [6], under suitable symmetry assumptions on the domain and on the boundary conditions. We confirm numerically that the crack growth is indeed intermittent, at least in those regimes where the plastic behavior cannot be neglected. Moreover, we provide examples which show the dependency of the number of jumps on the problem parameters.

ISSN 0944-6532 / $ 2.50 © Heldermann Verlag

Thanks to some symmetry assumptions, the contribution of the plastic part of the problem reduces to a non-homogenous Neumann boundary condition on the cohesive portion of the crack path, which is itself an unknown of the problem (see Figure 2.2).

When considering a rectangular domain and prescribing a straight crack path, we prove that the cohesive zone is a segment, and we provide a constructive way to identify the coordinates of the end points of this segment. This is done by solving a series of standard Laplace equations in the rest of the domain in order to minimize a suitable energy with respect to the coordinates of the end points. The presented strategy allows us to avoid the typical difficulties that are present in the solution of classical minimization problems of elasto-plasticity.

## 2. Formulation of the problem

We consider a simplified quasi-static model of crack growth in elasto-plastic materials, in the discrete time formulation with prescribed crack path. Our model is antiplane, with reference configuration given by the rectangle

$$\Omega := (0, a) \times (-b, b), \tag{1}$$

for some $a > 0$ and $b > 0$.

Given $T$ and $n$, let $t_i := iT/n$, $i = 0, \dots, n$ be a discrete sampling of the time interval $[0, T]$. The displacement at time $t_i$ is given by a scalar function $u_i \colon \Omega \to \mathbb{R}$, which takes a prescribed value on the Dirichlet part of the boundary, given by

$$\partial_D \Omega := [0, a] \times \{-b, b\}. \tag{2}$$

Namely, we assume that at time $t_i$

$$u_i(x, \pm b) = \pm w_i(x) \quad \text{for every } x \in (0, a), \tag{3}$$

where the functions $w_i \colon [0, a] \mapsto \mathbb{R}$ satisfy the following three conditions:

$$w_i \in C^\infty([0, a]) \text{ and is not identically zero for } i = 0, 1, \dots, n, \tag{4}$$

$$0 \le w_{i-1} \le w_i \quad \text{on } [0, a] \text{ for } i = 1, \dots, n, \tag{5}$$

$$w_i \text{ is nonincreasing and nonnegative on } [0, a] \text{ for } i = 0, 1, \dots, n. \tag{6}$$

The crack path is the segment

$$\Gamma := [0, a] \times \{0\}, \tag{7}$$

and in our model we assume also that the plastic strain is concentrated on $\Gamma$. For convenience, we indicate the set $[s_1, s_2] \times \{0\}$ with $\Gamma_{s_1}^{s_2}$.

The crack at time $t_i$ has the form $\Gamma_0^{s_i}$ for some $s_i \in [0, a]$, which represents the position of the crack tip. Since the plastic strain is concentrated on $\Gamma$, for every $t_i$ the corresponding displacement $u_i$ belongs to $H^1(\Omega \setminus \Gamma)$. The plastic slip is localized on $\Gamma_{s_i}^a$ and is given by $[u_i]$, where, for every $v \in H^1(\Omega \setminus \Gamma)$, we set

$$[v](x) = \lim_{y \to 0^+} \big(v(x, y) - v(x, -y)\big)$$

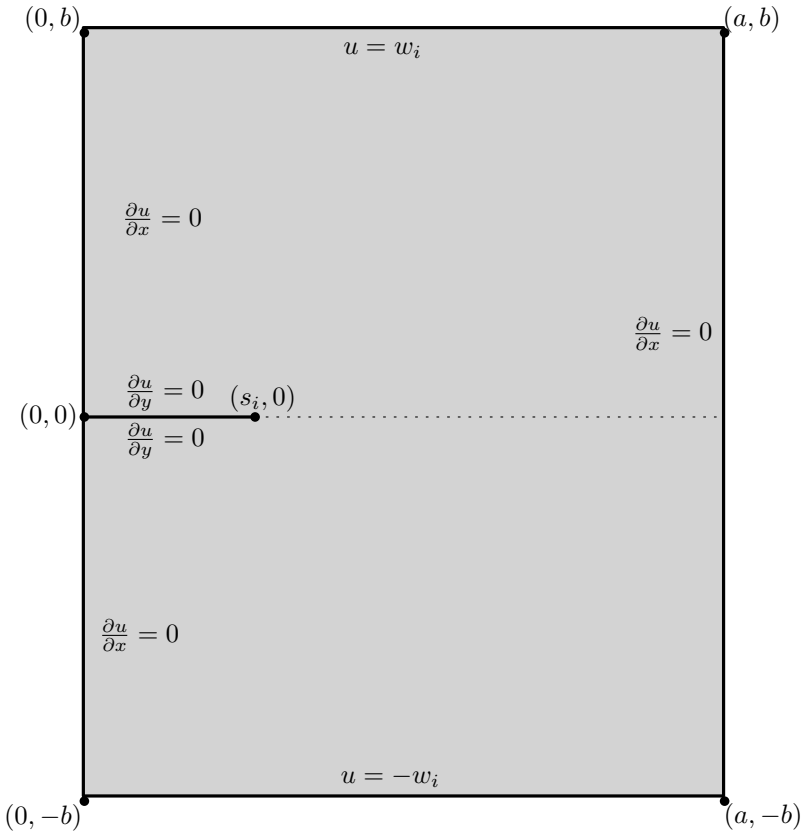


Figure 2.1: Schematic of the domain, boundary conditions, and crack tip position.

in the sense of traces. We refer to Figure 2.1 for a schematic of the domain and of the boundary conditions.

We consider a model where the stored elastic energy at time $t_i$ is given by

$$\mathcal{E}_i^e := \frac{\alpha}{2} \int_{\Omega \setminus \Gamma} |\nabla u_i|^2 \, \mathrm{d}x \, \mathrm{d}y, \tag{8}$$

the plastic dissipation distance between $u_{i-1}$ and $u_i$ is given by

$$\mathcal{E}_i^p := \beta \int_{\Gamma_{s_i}^a} |[u_i] - [u_{i-1}]| \, \mathrm{d}x, \tag{9}$$

while the energy dissipated by the crack growth in the time interval between $t_{i-1}$ and $t_i$ is given by

$$\mathcal{E}_i^c := \gamma(s_i - s_{i-1}). \tag{10}$$

Here and henceforth $\alpha$, $\beta$, and $\gamma$ are positive material constants.

We assume that the initial condition $u_0$ for the displacement belongs to $H^1(\Omega)$ and satisfies

$$\begin{cases} \Delta u_0 = 0 & \text{in } \Omega\,, \\ u_0(\cdot, \pm b) = \pm w_0 & \text{on } (0,a)\,, \\ \frac{\partial u_0}{\partial x}(0,\cdot) = \frac{\partial u_0}{\partial x}(a,\cdot) = 0 & \text{on } (-b,b)\,. \end{cases} \tag{11}$$

Let $s_0 \in (0,a)$ be the initial condition for the crack tip. In our model, the pair $(u_i, s_i)$, with $i = 1, \dots, n$, is obtained inductively as a solution of the minimum problem

$$\min_{\substack{u\in H^1(\Omega\setminus\Gamma)\\ u=w_i \text{ on } \partial_D\Omega\\ s_{i-1}\le s\le a}} \left\{\frac{\alpha}{2}\int_{\Omega\setminus\Gamma} |\nabla u|^2 \,\mathrm{d}x\,\mathrm{d}y + \beta\int_{\Gamma_s^a} |[u]-[u_{i-1}]|\,\mathrm{d}x + \gamma(s-s_{i-1})\right\}. \tag{12}$$

In general this solution is not unique, but two solutions with the same value of $s$ must coincide by strict convexity in $u$. By considering the Euler equation of (12) we see that the second term produces a cohesive force equal to $\pm\beta$ at the points of $\Gamma_s^a$ where $\pm([u]-[u_{i-1}]) < 0$.

Due to the symmetry of the data we shall work in $\Omega^+ := (0,a)\times(0,b)$ with Dirichlet boundary conditions on $\partial_D^+\Omega := [0,a]\times\{b\}$. This is justified by the following remark.

**Remark 2.1.** Since the boundary condition (3) is odd with respect to $y$, a pair $(u_i, s_i)$ is a solution of (12) if and only if $u_i$ is odd with respect to $y$ and $(u_i|_{\Omega^+}, s_i)$ is a solution of the minimum problem

$$\min_{\substack{u\in H^1(\Omega^+)\\ u=w_i \text{ on } \partial_D^+\Omega\\ s_{i-1}\le s\le a}} \left\{\frac{\alpha}{2}\int_{\Omega^+} |\nabla u|^2 \,\mathrm{d}x\,\mathrm{d}y + \beta\int_{\Gamma_s^a} |u-u_{i-1}|\,\mathrm{d}x + \frac{\gamma}{2}(s-s_{i-1})\right\}. \tag{13}$$

Moreover, $u_0$ is odd with respect to $y$ and $u_0|_{\Omega^+}$ is the solution of the boundary value problem

$$\begin{cases} \Delta u = 0 & \text{in } \Omega^+\,,\\ u = w_0 & \text{if } y = b\,,\\ \frac{\partial u}{\partial x} = 0 & \text{if } x = 0 \text{ or } x = a\,,\\ u = 0 & \text{if } y = b\,. \end{cases} \tag{14}$$

To solve (13), for every $s_{i-1} \le s \le a$ we find the unique solution $u_i^s$ of the problem

$$\min_{\substack{u\in H^1(\Omega^+)\\ u=w_i \text{ on } \partial_D^+\Omega}} \left\{\frac{\alpha}{2}\int_{\Omega^+} |\nabla u|^2 \,\mathrm{d}x\,\mathrm{d}y + \beta\int_{\Gamma_s^a} |u-u_{i-1}|\,\mathrm{d}x\right\}, \tag{15}$$

and then we find a value $s_i$ of $s$ which solves the minimum problem

$$\min_{s_{i-1}\le s\le a} \left\{\frac{\alpha}{2}\int_{\Omega^+} |\nabla u_i^s|^2 \,\mathrm{d}x\,\mathrm{d}y + \beta\int_{\Gamma_s^a} |u_i^s-u_{i-1}|\,\mathrm{d}x + \frac{\gamma}{2}(s-s_{i-1})\right\}. \tag{16}$$

The pair $(u_i, s_i)$, with $u_i := u_i^{s_i}$, is a solution of (13).

The solution of (15) will be constructed by using the solutions of some auxiliary boundary value problems for the Laplace equation, depending on a parameter $\sigma$, and then by choosing a particular value $\sigma_i^s$ of this parameter. Let us fix $s \in [s_0, a]$.

For every $\sigma \in [s,a]$ we consider the solution $u_i^{s,\sigma} \in H^1(\Omega^+)$ of the problem (see Figure 2.2)

$$\begin{cases} \Delta u = 0 & \text{in } \Omega^+, \\ u = w_i & \text{if } y = b\,, \\ \frac{\partial u}{\partial x} = 0 & \text{if } x = 0 \text{ or } x = a\,, \\ \frac{\partial u}{\partial y} = 0 & \text{for } 0 < x < s \text{ and } y = 0\,, \\ \frac{\partial u}{\partial y} = \frac{\beta}{\alpha} & \text{for } s < x < \sigma \text{ and } y = 0\,, \\ u = 0 & \text{for } \sigma < x < a \text{ and } y = 0\,. \end{cases} \tag{17}$$

By the continuous dependence on the data, the function $u_i^{s,\sigma}$ is continuous in $H^1(\Omega^+)$ with respect to $\sigma$.

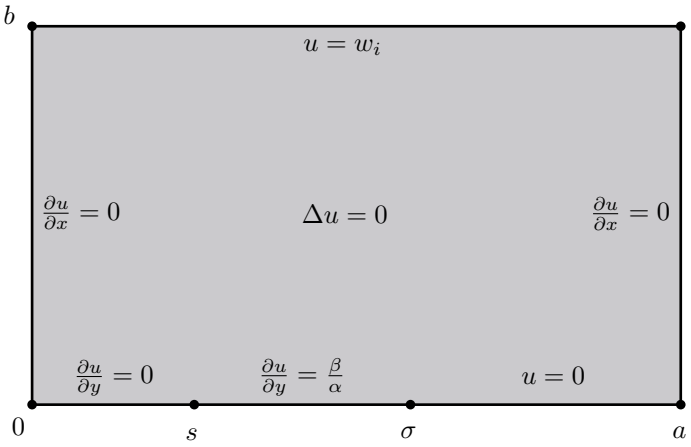


Figure 2.2: The boundary value problem for $u_i^{s,\sigma}$.

We define
$$\sigma_i^s := \max\{\sigma \in [s,a] : u_i^{s,\sigma} \geq 0 \text{ in } \Omega^+\}. \tag{18}$$
The existence of the maximum follows easily from the continuous dependence of $u^{s,\sigma}$ on $\sigma$. We shall prove that the solution $u_i^s$ of (15) is given by

$$u_i^s = u_i^{s,\sigma}\,, \text{ with } \sigma = \sigma_i^s. \tag{19}$$

**Remark 2.2.** By the maximum principle the inequality $u_i^{s,\sigma} \geq 0$ in $\Omega^+$ is satisfied if and only if the trace of $u_i^{s,\sigma}$ satisfies $u_i^{s,\sigma}(x,0) \geq 0$ for every $x \in (s,\sigma)$. Therefore we have

$$\sigma_i^s := \max\{\sigma \in [s,a] : u_i^{s,\sigma}(x,0) \geq 0 \text{ for every } x \in (s,\sigma)\}\,. \tag{20}$$

The following lemmas shows the connection between the minimum problem (15) and the functions $u_i^{s,\sigma}$.

**Lemma 2.3.** *Let $s \in [s_0,a)$, $i = 1,\dots,n$, let $u_i^{s,\sigma}$ be defined as in* (17)*, with $\sigma = \sigma_i^s$ defined as in* (18)*, and let $z \in H^1(\Omega^+)$ be such that $0 \leq z \leq u_i^{s,\sigma}$ a.e. on $\Gamma_s^a$. Then $u_i^{s,\sigma}$ is the solution of the minimum problem*

$$\min_{\substack{u \in H^1(\Omega^+) \\ u = w_i \ \text{on} \ \partial_D^+\Omega}} \left\{ \frac{\alpha}{2} \int_{\Omega^+} |\nabla u|^2 \,\mathrm{d}x\,\mathrm{d}y + \beta \int_{\Gamma_s^a} |u - z| \,\mathrm{d}x \right\}. \tag{21}$$

**Proof.** The definition of $u_i^{s,\sigma}$ given here differs from the definition in [6, formula (5.15)] only in the boundary condition at $y = b$, which is now the nondecreasing function $w_i$. The proof in our case can be obtained by repeating the proofs of Lemmas 5.7, 5.8, 5.9, and 5.11 of [6], with minor changes. In particular, the assumption that $w_i$ is nonincreasing is used in the proof of Lemma 5.7, where the $C^\infty$-regularity of $u_i^{s,\sigma}$ at the vertices $(0, b)$ and $(a, b)$ cannot be obtained for a nonconstant $w_i$, with no consequences on the conclusion. □

We now want to prove that the solution $u_i^s$ of problem (15) is given by $u_i^s = u_i^{s,\sigma}$, with $\sigma = \sigma_i^s$, where $u_i^{s,\sigma}$ is defined by (17) and $\sigma_i^s$ by (18). This will be a consequence of Lemma 2.3 if we show that $u_{i-1} \le u_i^{s,\sigma}$ for $s \ge s_{i-1}$ and $\sigma = \sigma_i^s$. The tools to prove this inequality are given by the next lemma. For every $x$ and $y$ in $\mathbb{R}$, we set $x \vee y := \max\{x, y\}$ and $x \wedge y := \min\{x, y\}$.

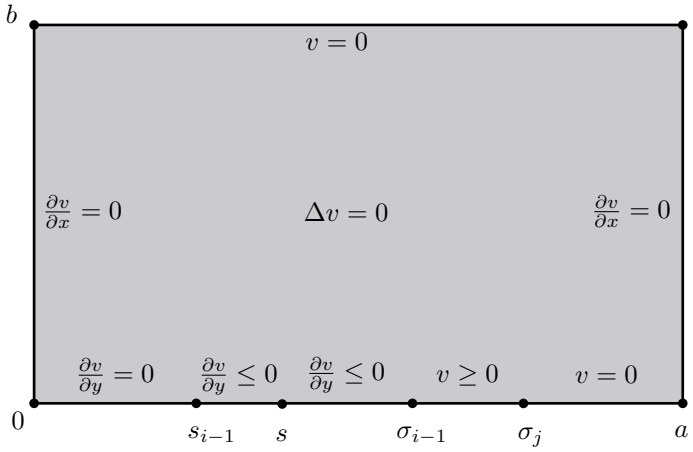


Figure 2.3: Boundary condition for $v$ when $s < \sigma_{i-1}$.

**Lemma 2.4.** *Let $i, j \in \{1, \dots, n\}$, with $i \le j$, and let $s \in [s_{i-1}, a]$, where $s_{i-1}$ is defined in* (13) *for $i \ge 2$. Then, setting $\sigma_{i-1} := \sigma_{i-1}^{s_{i-1}}$ and $\sigma_j := \sigma_j^s$ according to* (18)*, we have*

$$u_{i-1}^{s_{i-1},\sigma_{i-1}} \le u_j^{s,\sigma_j} \text{ in } \Omega^+ , \tag{22}$$

$$\sigma_{i-1} \le \sigma_j . \tag{23}$$

**Proof.** By the maximum principle we have

$$0 \le u_{i-1}^{s_{i-1},\sigma_{i-1}} \le u_j^{s_{i-1},\sigma_{i-1}} \quad \text{in } \Omega^+, \tag{24}$$

where we compare two solutions of problem (17), with $s = s_{i-1}$, and $\sigma = \sigma_{i-1}$, changing only the boundary condition from $w_{i-1}$ to $w_j$, which satisfy $w_{i-1} \le w_j$ by (5). To prove (22) it is enough to show that

$$u_j^{s_{i-1},\sigma_{i-1}} \le u_j^{s,\sigma_j} \text{ in } \Omega^+ . \tag{25}$$

Let $v := u_j^{s,\sigma_j} - u_j^{s_{i-1},\sigma_{i-1}}$. Then $v \in H^1(\Omega^+)$ and $\Delta v = 0$ in $\Omega^+$. See Figure 2.3 for a schematic of the boundary conditions satisfied by $v$, that will be explained below.

Since $u_j^{s,\sigma_j} = u_j^{s_{i-1},\sigma_{i-1}} = w_j$ for $y = b$, we have $v = 0$ for $y = b$. The equalities $\frac{\partial}{\partial x} u_j^{s,\sigma_j} = \frac{\partial}{\partial x} u_j^{s_{i-1},\sigma_{i-1}} = 0$ for $x = 0$ or $x = a$ give

$$\frac{\partial v}{\partial x} = 0 \quad \text{for} \quad x = 0 \text{ or } x = a\,. \tag{26}$$

Since $u_j^{s_{i-1},\sigma_{i-1}} \geq 0$ in $\Omega^+$ by (24) and $u_j^{s_{i-1},\sigma_{i-1}} = 0$ for $\sigma_{i-1} < x < a$ and $y = 0$ by (17), we have $\frac{\partial}{\partial y} u_j^{s_{i-1},\sigma_{i-1}} \geq 0$ for $\sigma_{i-1} < x < a$ and $y = 0$. By (17) we have also $\frac{\partial}{\partial y} u_j^{s_{i-1},\sigma_{i-1}} = 0$ for $0 < x < s_{i-1}$ and $y = 0$ and $\frac{\partial}{\partial y} u_j^{s_{i-1},\sigma_{i-1}} = \frac{\beta}{\alpha}$ for $s_{i-1} < x < \sigma_{i-1}$ and $y = 0$, hence $\frac{\partial}{\partial y} u_j^{s_{i-1},\sigma_{i-1}} \geq 0$ for $x \in (0,a) \setminus \{s_{i-1}, \sigma_{i-1}\}$ and $y = 0$. Since $\frac{\partial}{\partial y} u_j^{s,\sigma_j} = 0$ for $0 < x < s$ and $y = 0$ by (17), the previous inequality gives

$$\frac{\partial v}{\partial y} \leq 0 \text{ for } x \in (0,s) \setminus \{s_{i-1}, \sigma_{i-1}\} \text{ and } y = 0\,. \tag{27}$$

By [6, Lemma 5.9], which is still valid with our definition of $u_j^{s,\sigma_j}$, we have $\frac{\partial}{\partial y} u_j^{s,\sigma_j} \leq \frac{\beta}{\alpha}$ for $\sigma_j < x < a$ and $y = 0$. Since $\frac{\partial}{\partial y} u_j^{s,\sigma_j} = \frac{\beta}{\alpha}$ for $s < x < \sigma_j^s$ and $y = 0$ by (17), we have $\frac{\partial}{\partial y} u_j^{s,\sigma_j} \leq \frac{\beta}{\alpha}$ for $x \in (s,a) \setminus \{\sigma_j\}$ and $y = 0$. Using the equality $\frac{\partial}{\partial y} u_j^{s_{i-1},\sigma_{i-1}} = \frac{\beta}{\alpha}$ for $s_{i-1} < x < \sigma_{i-1}$ and $y = 0$, given by (17), we deduce that

$$\frac{\partial v}{\partial y} \leq 0 \text{ for } x \in (s, s \vee \sigma_{i-1}) \setminus \{\sigma_j\} \text{ and } y = 0\,. \tag{28}$$

Since $u_j^{s,\sigma_j} \geq 0$ for $x \in (0,a) \setminus \{s, \sigma_j\}$ and $y = 0$ by (18), while $u_j^{s_{i-1},\sigma_{i-1}} = 0$ for $\sigma_{i-1} < x < a$ and $y = 0$ by (17), we have

$$v \geq 0 \text{ for } x \in (s \vee \sigma_{i-1}, a) \setminus \{\sigma_j\} \text{ and } y = 0\,. \tag{29}$$

We now prove that, using a suitable version of the maximum principle, the boundary conditions discussed above (see Figure 2.3) imply that $v \geq 0$ in $\Omega^+$. Let $\varphi \in H^1(\Omega^+)$ with $\varphi = 0$ for $y = b$ and for $s \vee \sigma_{i-1} < x < a$ and $y = 0$. Suppose in addition that $\varphi$ vanishes in a neighborhood of the vertices of the rectangle $\Omega^+$ and of the points $(s_{i-1}, 0)$, $(\sigma_{i-1}, 0)$, $(s, 0)$, $(\sigma_j, 0)$.

Since $\int_{\Omega^+} \Delta v \varphi \, \mathrm{d}x \, \mathrm{d}y = 0$, integrating by parts from (26) we obtain the weak formulation

$$\int_{\Omega^+} \nabla v \nabla \varphi \, \mathrm{d}x \, \mathrm{d}y = -\int_{\Gamma_0^{s \vee \sigma_{i-1}}} \frac{\partial v}{\partial y} \varphi \, \mathrm{d}x \tag{30}$$

Since points have capacity zero, every function in $H^1(\Omega^+)$ can be approximated in $H^1(\Omega^+)$ by functions that vanish in a neighborhood of a prescribed finite set of points. Therefore (30) holds for every $\varphi \in H^1(\Omega^+)$ with $\varphi = 0$ for $y = b$ and for $s \vee \sigma_{i-1} < x < a$ and $y = 0$. Taking $\varphi := v \wedge 0$ we obtain

$$\int_{\Omega^+} |\nabla (v \wedge 0)|^2 = \int_{\Omega^+} \nabla v \nabla (v \wedge 0) \, \mathrm{d}x \, \mathrm{d}y = -\int_{\Gamma_0^{s \vee \sigma_{i-1}}} \frac{\partial v}{\partial y} (v \wedge 0) \, \mathrm{d}x\,.$$

Since $\frac{\partial v}{\partial y} \leq 0$ a.e. in $\Gamma_0^{s\vee\sigma_{i-1}}$ by (26)–(28), the right-hand side of the previous equality is less than or equal to 0, which gives $\nabla(v \wedge 0) = 0$ in $\Omega^+$. Taking into account the boundary condition $v = 0$ on $\partial_D^+\Omega$ we get $v \wedge 0 = 0$ in $\Omega^+$. This implies $v \geq 0$, which proves (25).

Property (23) is trivial if $\sigma_{i-1} \leq s$, since $s \leq \sigma_j$ by (18). If $s < \sigma_{i-1}$ inequality (23) follows from (18) and from the inequality $u_{i-1}^{s_{i-1},\sigma_{i-1}} \leq u_j^{s,\sigma_{i-1}}$, which can be proved by adapting the argument used in the proof of the inequality $v \geq 0$. □

We are now able to prove the result which allows us to construct the solution of the minimum problems (15) by means of the solutions of (17).

**Lemma 2.5.** *Assume that* (4)–(6) *hold. Then for every* $i = 1, \ldots, n$ *and every* $s_{i-1} \leq s \leq a$ *the solution* $u_i^s$ *of the minimum problem* (15) *coincides with the function* $u_i^{s,\sigma}$ *defined in* (17)*, with boundary data* $w_i$ *and with* $\sigma = \sigma_i^s$ *defined in* (18)*.*

**Proof.** The proof is obtained by induction on $i$ using Lemmas 2.3 and 2.4. Since $u_0$ satisfies (14), for every $s_0 \leq s \leq a$ by (18) we have $u_0 = 0 \leq u_1^{s,\sigma}$ for $y = 0$ and $\sigma = \sigma_1^s$, while $0 \leq u_0 = w_0 \leq w_1 = u_1^{s,\sigma}$ for $y = 0$ and $\sigma = \sigma_1^s$ by (5). Using the comparison principle we obtain $0 \leq u_0 \leq u_1^{s,\sigma}$in $\Omega^+$ for $s_0 \leq s \leq a$ and $\sigma = \sigma_1^s$. Then $u_1^s = u_1^{s,\sigma}$ with $\sigma = \sigma_1^s$ by Lemma 2.3 with $z = u_0$.

Assume now that the statement of the Lemma is true for step $i - 1$. Then in particular $u_{i-1} = u_{i-1}^{s_{i-1}} = u_{i-1}^{s_{i-1},\sigma}$ with $\sigma = \sigma_{i-1}^{s_{i-1}}$. The statement of the Lemma for step $i$ follows from Lemma 2.3, applied with $z = u_{i-1}$. We see that the hypothesis of Lemma 2.3 are satisfied using Lemma 2.4 with $j = i$. □

## 3. Finite element approximation

In order to provide a numerical approximation to problem (13), we fix a family $\{\mathcal{T}_h(\Omega^+)\}_{h>0}$ of conforming subdivisions of $\overline{\Omega}^+$ made of quadrilaterals, with $h$ denoting their maximal size. We assume that $\mathcal{T}_h(\Omega^+)$ are shape-regular and quasi-uniform in the sense of [4, 9], and that they contain the point $(s_0, 0)$ among their vertices. Each subdivision $\mathcal{T}_h(\Omega^+)$ induces a discrete set $\mathcal{S}_h$ in the segment $[s_0, a] \times \{0\}$, composed of all vertices of $\mathcal{T}_h$ that belong to $[s_0, a] \times \{0\}$.

Given $s$, $\sigma \in \mathcal{S}_h$ with $s \leq \sigma$, we first consider a finite element approximation of the auxiliary problem (17).

Let $\mathbb{V}_h$ denote the subspace of $H^1(\Omega^+)$ continuous piecewise bi-linear functions subordinate to $\mathcal{T}_h(\Omega^+)$, and let $I_h : H^1(\Omega^+) \to \mathbb{V}_h$ be the Scott-Zhang interpolation [17] which has the following approximation property

$$\|v - I_h v\|_{H^1(\Omega^+)} \leq C_{r,\Omega^+} h^r \|v\|_{H^{1+r}(\Omega^+)}, \quad \text{for } v \in H^{1+r}(\Omega^+), \tag{31}$$

where $C_{r,\Omega^+}$ depends on $r$, $\Omega^+$, and on the shape regularity of $\mathcal{T}_h$, but is independent of $h$.

Let $\mathbb{V}_0^\sigma$ be the space of test functions in $H^1(\Omega^+)$ whose trace vanish on $\Gamma_\sigma^a$ and on $[0, a] \times \{b\}$, and let $\mathbb{V}_{h,0}^\sigma \subset \mathbb{V}_0$ be its discrete counterpart. Moreover, let $\mathbb{V}_w^\sigma$ be the the space of $H^1(\Omega^+)$ functions whose trace on $[0, a] \times \{b\}$ coincides with the function $w$ and that vanish on $\Gamma_\sigma^a$, and let $\mathbb{V}_{h,w}^\sigma$ be the space of their Scott-Zhang interpolation onto $\mathbb{V}_h^\sigma$.

The discrete counterpart of problem (17) then reads: Given the current boundary condition $w_i$, a crack tip opening $s \in \mathcal{S}_h$, and $\sigma \in \mathcal{S}_h$, with $s \le \sigma$, find $u_{i,h}^{s,\sigma} \in \mathbb{V}_{h,w_i}^{\sigma}$ satisfying

$$\int_{\Omega^+} \nabla u_{i,h}^{s,\sigma} \nabla v_h \,\mathrm{d}x\,\mathrm{d}y = \int_{\Gamma_s^\sigma} \frac{\beta}{\alpha} v_h \,\mathrm{d}x, \qquad \forall v_h \in \mathbb{V}_{h,0}^{\sigma}. \tag{32}$$

Since the subdivision $\mathcal{T}_h(\Omega^+)$ is conforming w.r.t. both $s$ and $\sigma$, i.e., both $s$ and $\sigma$ coincide with vertices of $\mathcal{T}_h(\Omega^+)$, then each term in (32) can be computed exactly, resulting in a symmetric and positive definite linear system of equations whose solution can be computed numerically using a standard preconditioned conjugate gradient method. By [6, Lemma 5.4 and Lemma 5.5], there exists $r \in (0,1)$ such that $u_i^{s,\sigma} \in H^{1+r}(\Omega^+)$, and we conclude that the numerical solution converges to the exact solution with the following estimate:

$$\|u_i^{s,\sigma} - u_{i,h}^{s,\sigma}\|_{H^1(\Omega^+)} \le C_{r,\Omega^+} h^r \|u_i^{s,\sigma}\|_{H^{1+r}(\Omega^+)}. \tag{33}$$

An approximate solution to problem (13) is then obtained by induction on $i$ through the solution of a series of auxiliary problems (32). To be precise, suppose that we know an approximate solution $(u_{i-1,h}, s_{i-1,h})$ of (13) at the time step $i-1$. To construct $(u_{i,h}, s_{i,h})$, we proceed as follows.

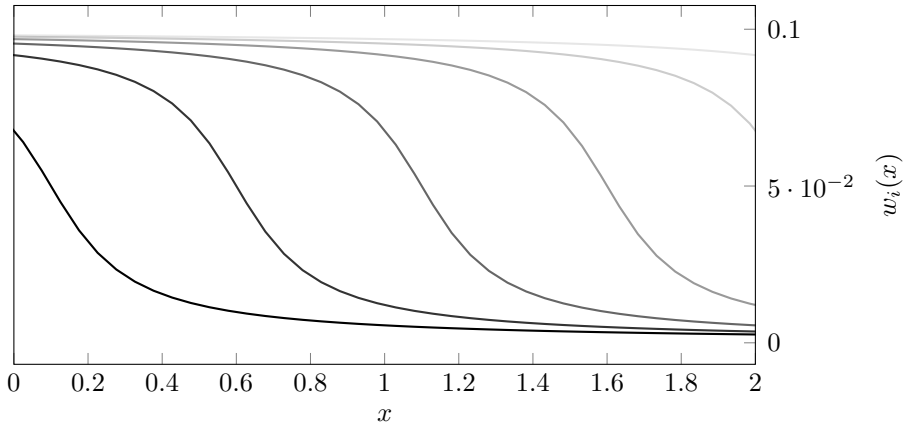


Figure 3.1: Evolution of the boundary condition $w_i$ for $t_i = 0, 0.5, 1.0, 1.5, 2.0, 2.5$, from left to right.

For any $s \in \mathcal{S}_h$ with $s \ge s_{i-1,h}$, we consider $\sigma_{i,h}^s$ the largest $\sigma \in \mathcal{S}_h$ such that $\sigma \ge s$ and $u_{i,h}^{s,\sigma} \ge 0$. Thanks to (23), it is enough to consider only $\sigma \ge s \vee \sigma_{i-1,h}^{s_{i-1,h}}$.

We set $u_{i,h}^s = u_{i,h}^{s,\sigma}$ with $\sigma = \sigma_{i,h}^s$. According to Lemma 2.5, $u_{i,h}^s$ can be considered as the discrete counterpart of the solution $u_i^s$ of problem (15).

The final step of our algorithm consists in finding a solution $s_{i,h} \in \mathcal{S}_h$ to the minimum problem

$$\min_{\substack{s \in \mathcal{S}_h \\ s \ge s_{i-1,h}}} \Big\{ \frac{\alpha}{2} \int_{\Omega^+} |\nabla u_{i,h}^s|^2 \,\mathrm{d}x\,\mathrm{d}y + \beta \int_{\Gamma_s^a} |u_{i,h}^s - u_{i-1,h}| \,\mathrm{d}x + \frac{\gamma}{2}(s - s_{i-1,h}) \Big\}.$$

The corresponding discrete solution at time index $i$ is given by $u_{i,h} := u_{i,h}^{s_{i,h}}$, so that the pair $(u_{i,h}, s_{i,h})$ can be considered as the discrete counterpart of the solution of problem (13).

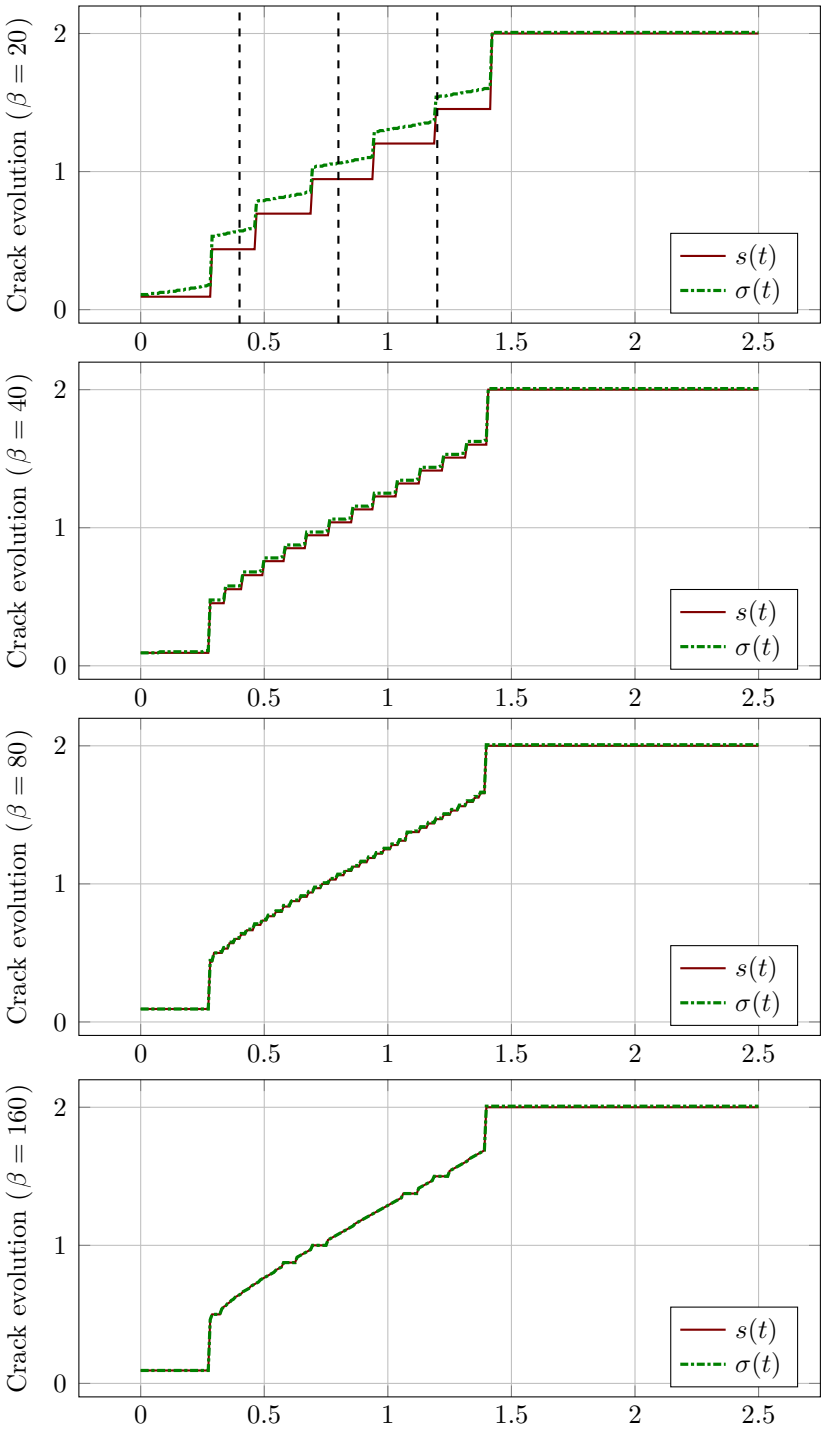


Figure 3.2: Crack fronts propagation for $\beta = 20, 40, 80$, and 160. The vertical dash lines in the plot for $\beta = 20$ show the times at which the solution is plotted in Figures 3.3 and 3.4.

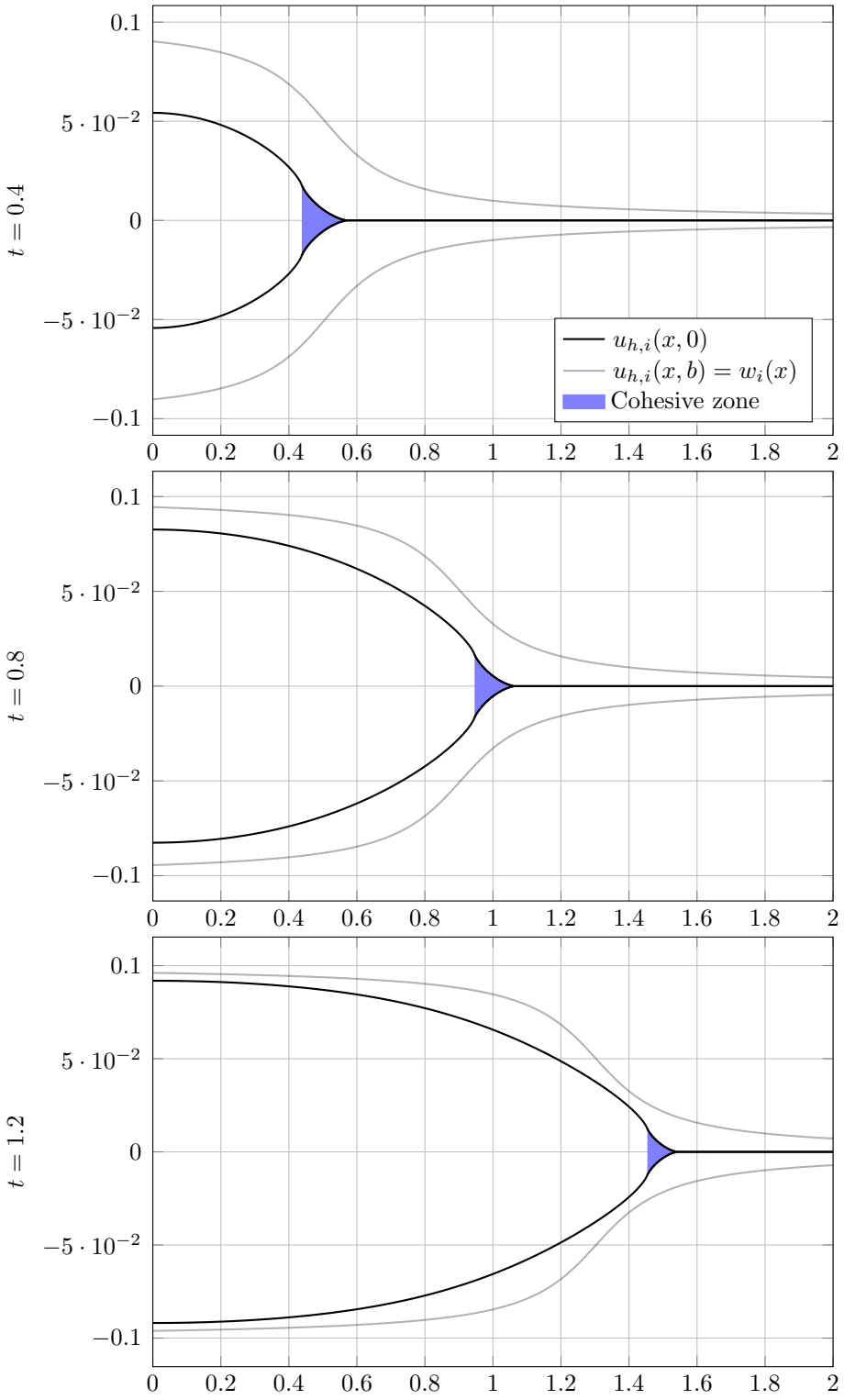


Figure 3.3: Solution at $y = 0$ and $y = 0.5$, for $t = 0.4, 0.8$, and $1.2$ for the case $\beta = 20$. The lower part is added by simmetry.

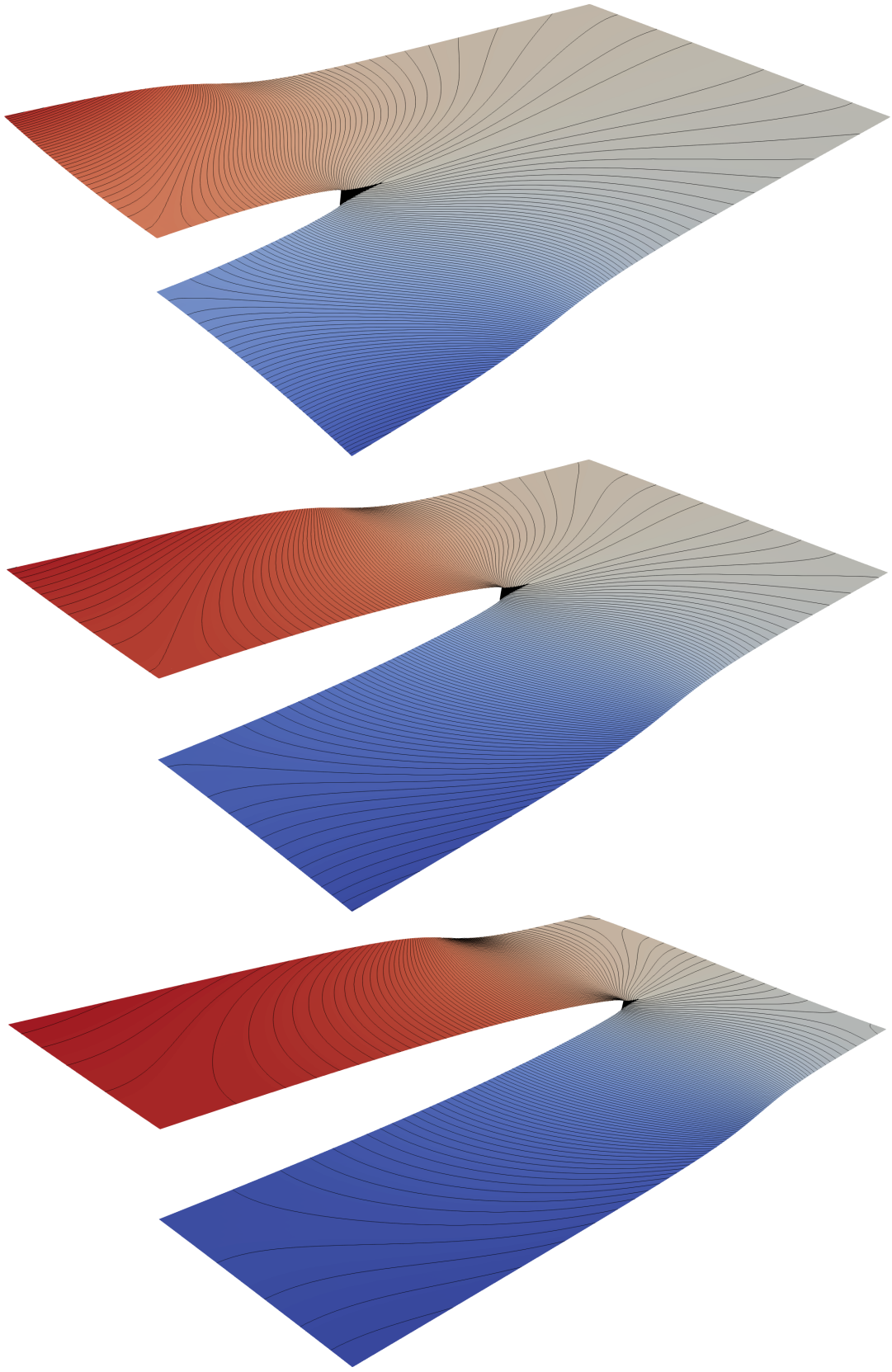

Figure 3.4: Antiplane representation of the solution at $t = 0.4, 0.8$, and $1.2$ for the case $\beta = 20$.

## 4. A numerical example

The example in this section has been implemented using the `deal.II` library [1, 2, 16]. We consider the domain $\Omega^+ = [0, a] \times [0, b]$, with $a = 2$ and $b = 0.5$, set the initial crack tip to $s_0 = 0.1$, and evolve the problem to a final time $T = 2.5$ for fixed values of $\alpha = 100$ and $\gamma = 0.5$, varying $\beta$ in the set $\{20, 40, 80, 160\}$. We consider the time dependent boundary condition

$$w_i(x) = c_1 \left( \frac{1}{2} - \frac{1}{\pi} \arctan \left( \frac{(x - t_i - s_0)c_2\pi}{c_1} \right) \right), \qquad i \geq 0\,, \tag{34}$$

for $c_1 = 0.1$ and $c_2 = 0.2$, which is shown in Figure 3.1 for some time steps, and set $u_0 = 0$.

Figure 3.2 shows clearly the jerky evolution of the crack tip when $\beta$ is small. As the value of $\beta$ increases, the crack tip evolves with more and more jumps, and the cohesive zone becomes smaller and smaller. When $\beta$ is very large, the evolution is essentially brittle, and the cohesive zone cannot be detected by the numerical algorithm. This is coherent with the results presented in [5, Subsection 8.2].

**Acknowledgements.** This paper is based on work supported by the National Research Projects (PRIN 2017) "Variational methods for stationary and evolution problems with singularities and interfaces", and "Numerical Analysis for Full and Reduced Order Methods for the efficient and accurate solution of complex systems governed by Partial Differential Equations", funded by the Italian Ministry of Education, University, and Research.

## References

[1] D. Arndt, W. Bangerth, T. C. Clevenger, D. Davydov, M. Fehling, D. Garcia-Sanchez, G. Harper, T. Heister, L. Heltai, M. Kronbichler, R. Maguire Kynch, M. Maier, J. P. Pelteret, B. Turcksin, D. Wells: *The deal.II library, Version 9.1*, J. Numer. Math. 27/4 (2019) 203–213.

[2] D. Arndt, W. Bangerth, D. Davydov, T. Heister, L. Heltai, M. Kronbichler, M. Maier, J.-P. Pelteret, B. Turcksin, D. Wells: *The deal.II finite element library: Design, features, and insights*, Comp. Math. Appl. 81 (2021) 407–422.

[3] S. Brach, E. Tanné, B. Bourdin, K. Bhattacharya: *Phase-field study of crack nucleation and propagation in elastic-perfectly plastic bodies*, Comp. Meth. Appl. Mech. Engineering 353 (2019) 44–65.

[4] P. G. Ciarlet: *The Finite Element Method for Elliptic Problems*, Classics in Applied Mathematics 40, SIAM, Philadelphia (2002).

[5] G. Dal Maso, R. Toader: *Quasistatic crack growth in elasto-plastic materials: The two-dimensional case*, Arch. Rational Mech. Analysis 196/3 (2010) 867–906.

[6] G. Dal Maso, R. Toader: *On the jerky crack growth in elastoplastic materials*, Calc. Var. Partial Diff. Equations 59 (2020), art. no. 107.

[7] L. De Lorenzis, A. McBride, B. D. Reddy: *Phase-field modelling of fracture in single crystal plasticity*, GAMM-Mitteilungen 39/1 (2016) 7–34.

[8] Y. Descatha, P. Ledermann, J. C. Devaux, F. Mudry, A. Pineau, J. C. Lautridou: *Experimental and numerical study of the different stages in ductile rupture – Application*

*to crack initiation and stable crack growth*, Three-dimensional constitutive relations and ductile fracture (A 83-18477 06-39), North-Holland Publishing Co., Amsterdam (1981) 185–205.

[9] A. Ern, J.-L. Guermond: *Theory and Practice of Finite Elements*, Applied Mathematical Sciences 159, Springer, Berlin (2004).

[10] D. Hull: *Fractography Observing, Measuring and Interpreting Fracture Surface Topography*, Cambridge Univerty Press, Cambridge (1999).

[11] J. W. Hutchinson: *A Course on Nonlinear Fracture Mechanics*, Department of Solid Mechanics, Technical University of Denmark (1979).

[12] A. Mielke, T. Roubiček: *Rate-Independent Systems. Theory and Application*, Springer, New York (2015).

[13] M. Ortiz, A. Pandolfi: *Finite-deformation irreversible cohesive elements for three-dimensional crack-propagation analysis*, Int. J. Numer. Meth. Engineering 44/9 (1999) 1267–1282.

[14] J. R. Rice: *Mathematical analysis in the mechanics of fracture*, Math. Fundamentals 2/B2 (1968) 191–311.

[15] J. R. Rice, E. P. Sorensen: *Continuing crack-tip deformation and fracture for plane-strain crack growth in elastic-plastic solids*, J. Mech. Physics Solids 26/3 (1978) 163–186.

[16] A. Sartori, N. Giuliani, M. Bardelloni, L. Heltai: *deal2lkit: A toolkit library for high performance programming in deal.II*, SoftwareX 7 (2018) 318–327.

[17] L. R. Scott, S. Zhang: *Finite element interpolation of nonsmooth functions satisfying boundary conditions*, Math. Computation 54/190 (1990) 483.

[18] D. Wick, T. Wick, R. J. Hellmig, H.-J. Christ: *Numerical simulations of crack propagation in screws with phase-field modeling*, Comp. Materials Sci. 109 (2015) 367–379.